

Supporting Information for

Construction of micelles and hollow spheres from self-assembly behavior of poly(styrene-*alt*-*p*HPMI) copolymer with poly(4-vinylpyridine) derivatives mediated by hydrogen bonding interaction

Tzu-Ling Ma,^a Wei-Ting Du,^a and Shiao-Wei Kuo^{a,b*}

^aDepartment of Materials and Optoelectronic Science, Center of Crystal Research, National Sun Yat-Sen University, Kaohsiung 804, Taiwan.

^bDepartment of Medicinal and Applied Chemistry, Kaohsiung Medical University, Kaohsiung 807, Taiwan.

*Corresponding authors: E-mails: kuosw@faculty.nsysu.edu.tw

Characterization

FTIR spectra were measured with a Bruker Tensor 27 FTIR spectrophotometer and the conventional crystal KBr disk method was utilized: micelle solutions were cast onto the KBr disk, then dried in reduce pressure; 32 scans were collected at a spectral resolution of 4 cm^{-1} . $^1\text{H NMR}$ spectra were recorded using an INOVA 500 spectrometer in CDCl_3 , which as an external standard. Differential Scanning Calorimetry (DSC) was performed using a TA Q-20 analyzer. Glass transition temperatures were collected using ca. 5 mg sample placed on the DSC sample pan under a N_2 atmosphere (100 mL min^{-1}), then heated from 40 to $300\text{ }^\circ\text{C}$ at a heating rate of $10\text{ }^\circ\text{C min}^{-1}$. Thermogravimetric analysis (TGA) was carried out under N_2 atmosphere at a flow rate of 60 mL min^{-1} using a TA Q-50 analyzer to confirm the thermal stabilities of the samples, which were placed in a Pt cell and heated from 40 to $800\text{ }^\circ\text{C}$ at a heating rate of $20\text{ }^\circ\text{C min}^{-1}$. Molecular weights and Polydispersity indexes (M_w/M_n) were evaluated using GPC (Waters 510 gel permeation chromatograph). Particle sizes were estimated by dynamic light scattering instrument (DLS: NANOTRAC Wave II Q, Microtrac, MRB), which was conducted at $25\text{ }^\circ\text{C}$. Before the DLS examination, the mixture was filtrated through a syringe filter with $0.45\mu\text{m}$ porous size. The morphologies of the samples were examined through transmission electron microscopy (TEM), using a JEOL-2100 microscope operated at an accelerating voltage of 200 kV. Micelles solutions were dropped onto copper grids coated with carbon-supporting films. The specimens were dried in vacuum oven at ambient temperature, then stained with iodine (I_2) or ruthenium tetroxide (RuO_4). In TEM images, I_2 staining was selective for pyridine ring domain; RuO_4 staining was optional to pyridine ring and styrene domain, which corresponded to gray and dark contrasts respectively. Topological images of surface morphology were examined by using atomic force microscope (AFM),

equipped with a Hitachi High-Tech Instrument Scanning Probe Microscope (AFM5300E) and dynamic force mode. The specimens were prepared by a drop of micelles solution on a microscope slide and dried in a desiccator.

Polystyrene (PS)

Polystyrene was synthesized by free radical copolymerization. AIBN (5 wt%) was put in a 100-mL two-necked round-bottom flask, then dry THF (40 mL) was injected. When AIBN was thoroughly dissolved, then styrene (2.083 g, 0.02 mol) added into solution. The mixture reacted under N₂ at 70 °C and stirred for 24 h. Reaction was terminated by exposing to air for 1 h, then the solution was concentrated under reduced pressure until turbid. The final solutions were dropped into cold MeOH and the precipitates were purified with THF/cold MeOH twice. The white solid was dried under vacuum for 5 days. Yield: 0.488 g; FTIR (KBr, cm⁻¹): 3025 (Aromatic C–H stretching), 2924 (Alkanes C–H stretching), 1600 (Aromatic ring); ¹H NMR (500 MHz, chloroform-*d*, δ , ppm): 1.63–2.02 (3H, CH₂CH), 6.26–7.24 (5H, C=CH in aromatic rings); Thermal decomposition temperatures (T_{d5} and T_{d10}) were 339 and 377 °C; Number-average molecular weight M_n : ca. 9,421 g mol⁻¹, polydispersity index (PDI): 1.137.

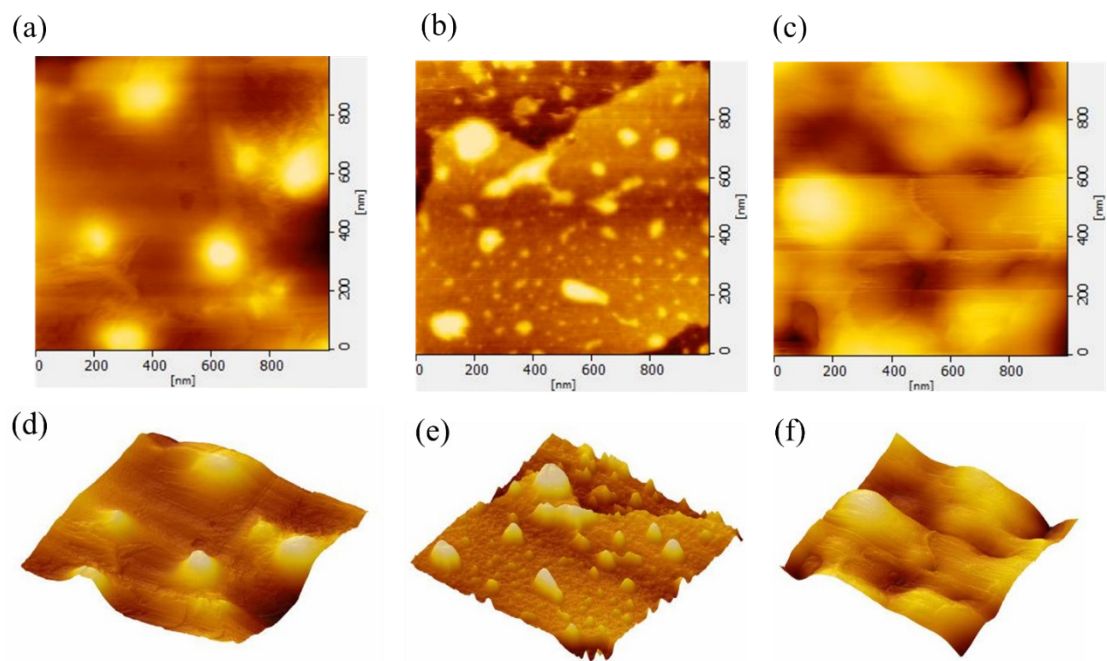


Figure S1: AFM images of (a–c) 2D topology and (d–f) 3D topology images of (a, d) hydrogen bonding connected micelles, (b, e) crosslinked micelles with 1,4-dibromobutane, and (c, f) the hollow spheres after dissolution in DMF solution from poly(*S-alt-p*HPMI)/P4VP inter-polymer complex

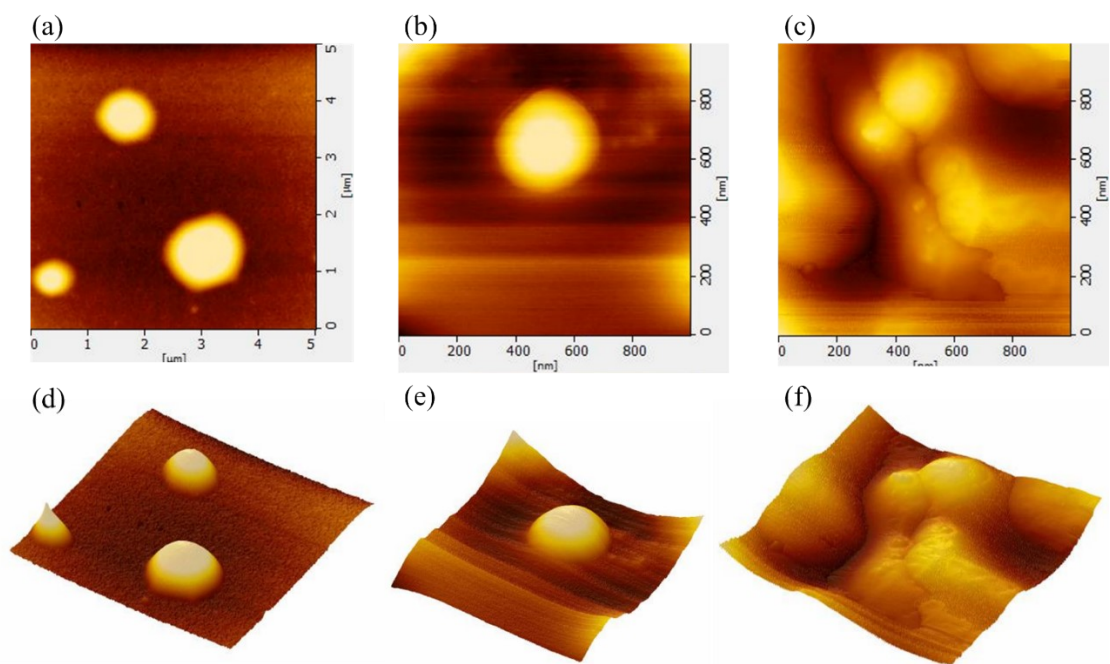


Figure S2: AFM images of (a–c) 2D topology and (d–f) 3D topology images of (a, d) hydrogen bonding connected micelles, (b, e) crosslinked micelles with 1,4-dibromobutane, and (c, f) the hollow spheres after dissolution in DMF solution from poly(*S-alt-p*HPMI)/PS₄₁-*r*-P4VP₅₉ inter-polymer complex

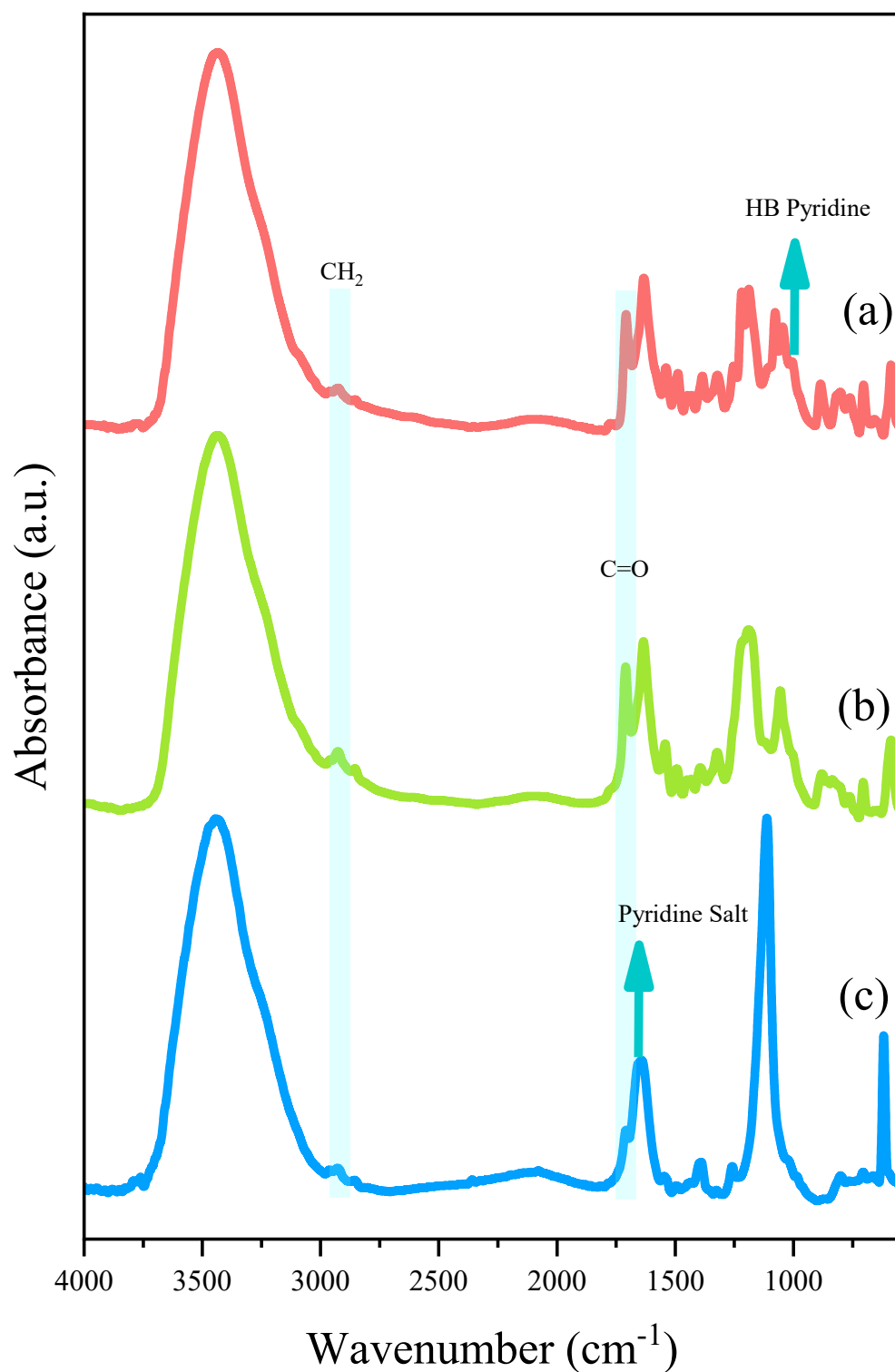


Figure S3: FTIR spectra of (a) hydrogen bonding connected micelles, (b) cross-linked micelles with 1,4-dibromobutane, and (c) the hollow spheres after dissolution in DMF solution from poly(*S-alt-p*HPMI)/PS_{41-*r*}-P4VP₅₉ inter-polymer complex

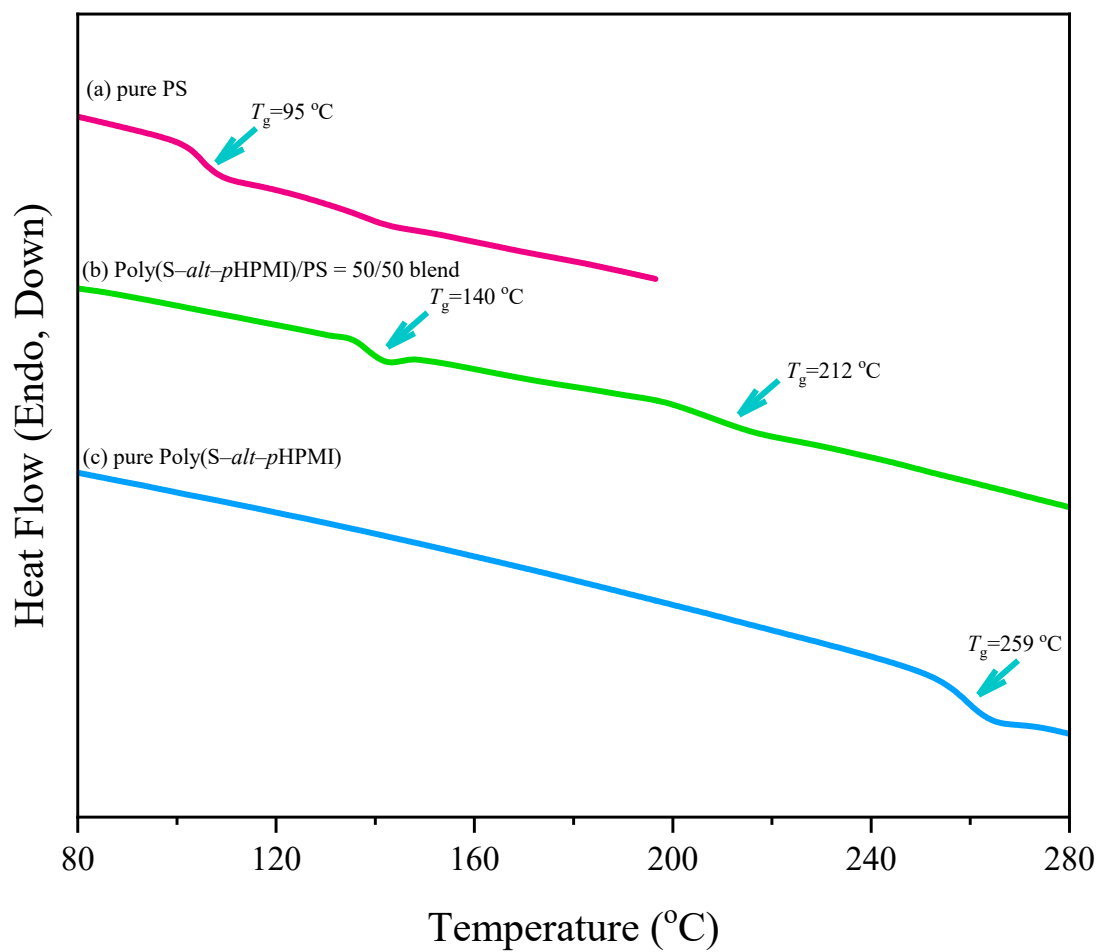


Figure S4: DSC thermal analyses of (a) pure PS, (b) poly(S-alt-pHPMI)/PS = 50/50 blend, (c) pure poly(S-alt-pHPMI)

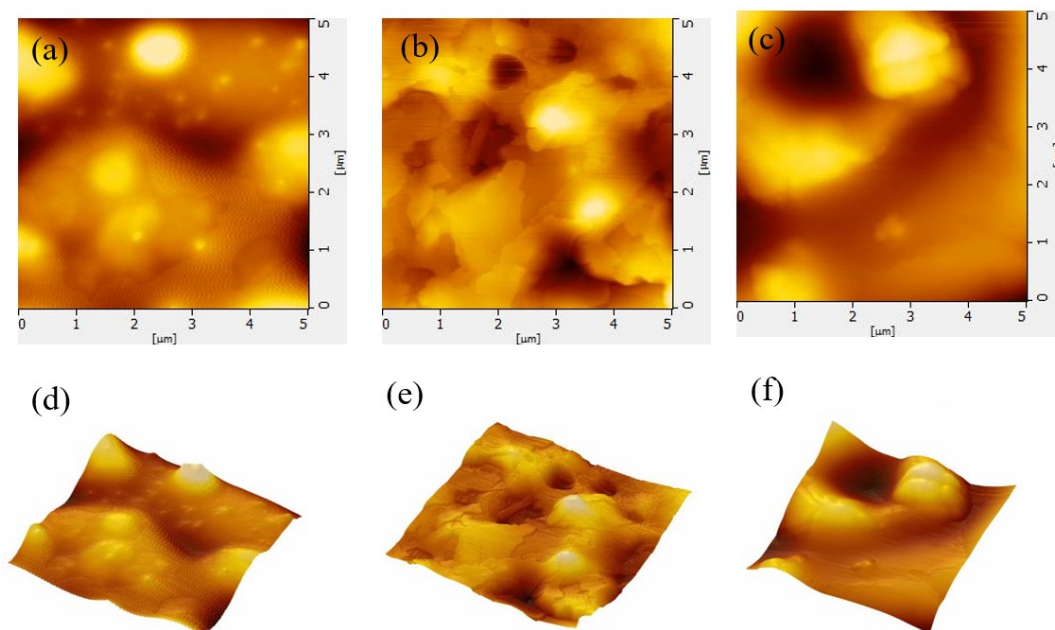


Figure S5: AFM images of (a–c) 2D topology and (d–f) 3D topology images of (a, d) hydrogen bonding connected micelles, (b, e) crosslinked micelles with 1,4-dibromobutane, and (c, f) the rod-like structures after dissolution in DMF solution from poly(*S-alt-p*HPMI)/PS₆₈-*b*-P4VP₃₂ inter-polymer complex

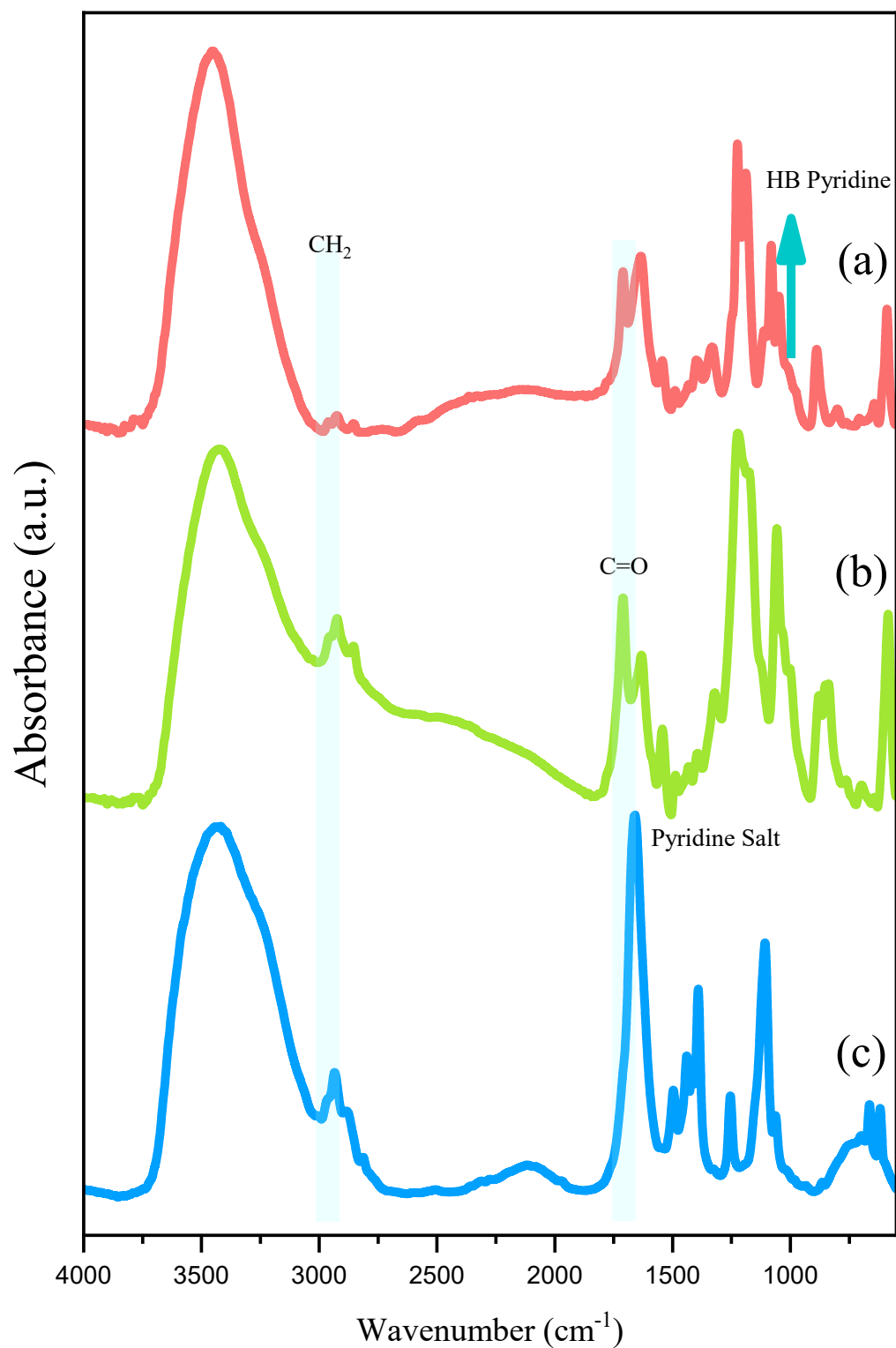


Figure S6: FTIR spectra of (a) hydrogen bonding connected micelles, (b) cross-linked micelles with 1,4-dibromobutane, and (c) the rod-like structures after dissolution in DMF solution from poly(*S-alt-p*HPMI)/PS₆₈-*b*-P4VP₃₂ inter-polymer complex